Thermo-economic optimization of small-scale organic Rankine cycle: A case study for low-grade industrial waste heat recovery

Bernardo Peris[1, a, b], Joaquín Navarro-Esbrí [b], Carlos Mateu-Royo [b], Adrián Mota-Babiloni [b], Francisco Molés [b, c], Antonio J. Gutiérrez-Trashorras [d], Marta Amat-Albuixech [b]

[a] Grupo de Termotecnia, Energetic Engineering Department, Escuela Técnica Superior de Ingeniería, Universidad de Sevilla, Camino de los Descubrimientos s/n, 41092 Sevilla, Spain

[b] ISTENER Research Group, Department of Mechanical Engineering and Construction, Universitat Jaume I, Campus de Riu Sec s/n, 12071 Castelló de la Plana, Spain

[c] Expander Tech S.L. (Rank), 12600 La Vall d'Uixó, Spain

[d] Ingeniería Fluidodinámica GIFD, Energy Department, Escuela Politécnica de Ingeniería, Edificio de Energía, Universidad de Oviedo, Campus de Viesques, 33203 Gijón, Asturias, Spain

Abstract

This work is focused on a case study of a small-scale Organic Rankine Cycle (ORC) adopted for electricity production from low-grade industrial waste heat recovery. This kind of applications raises a great interest due to the high amount of low-grade waste heat recoverable within industrial processes, but lacks of in-depth experimental investigations on the topic. The main reason is the difficulty to reach profitable small-scale projects, so more cost-effective solutions are being explored in the literature through thermo-economic optimizations. Nonetheless, the results obtained cannot be discussed with respect to actual operating data. In light of this, this paper proposes to conduct the thermo-economic optimization on the basis of an experimental application. In this manner, a comprehensive model of the facility is developed, calibrated, and validated from actual operating data. The model is used to conduct the thermo-economic optimization, revealing the influence of the organic fluid, cycle architecture, geometric parameters of main components, or control strategy used to obtain the best cost-effective solution. The main results show that, by means of a multivariable optimization using cost-effective ratios as objective function, a cheaper and powerful solution adapted to each specific project may be designed.

Keywords: energy efficiency; thermodynamic model; volumetric expander; low global warming potential working fluid; experimental analysis.

Acronyms	
GWP	Global Warming Potential
HCFO	Hydrochlorofluoroolefin
HFC	Hydrofluorocarbon
HFO	Hydrofluoroolefins
HRVG	Heat Recovery Vapor Generator
ORC	Organic Rankine Cycle
SIC	Specific Investment Cost (€/kW)
USD	United States Dollar
WHR	Waste Heat Recovery

[1] Corresponding Author:
Tel: +34 955420975
E-mail address: bperis@us.es

Nomenclature

A	Area (m^2)
Bo	Boiling number
C	Constant coefficient; Cost (€)
D	Diameter (m)
f	Friction factor
h	Convection coefficient ($kW \cdot m^{-2} \cdot K^{-1}$) ; Enthalpy ($kJ \cdot kg^{-1}$)
k	Thermal conductivity ($kW \cdot m^{-1} \cdot K^{-1}$)
L	Length (m)
M	Mass (kg)
$\dot{m}$	Mass flow rate ($kg \cdot s^{-1}$)
N	Number of a parameters
Nu	Nusselt number
P	Pressure (bar)
Pr	Prandtl number
Q	Thermal power (kW)
r	Radius (m)
Re	Reynolds number
s	Entropy ($kJ \cdot kg^{-1} \cdot K^{-1}$)
t	Thickness (m)
T	Temperature (ºC)
U	Uncertainty (%)
v	Velocity ($m \cdot s^{-1}$)
$\dot{V}$	Volumetric flow rate ($m^3 \cdot s^{-1}$)
V_r	Built-in volume ratio
W	Electric power (kW)

Greek symbols

β	Chevron angle (radians)
η	Efficiency (%)
ρ	Density ($kg \cdot m^{-3}$)
χ	Vapor dryness

Subscripts

cond	condenser
em	Electro-mechanical
eq	Equivalent
g	Gross
htl	Heat transfer loop
i	Input
ise	Isentropic
l	Liquid in saturated state
o	Output
p	Pump
Reg	Regenerator
s	Surface conditions
v	Vapor in saturated state; Volumetric (%)
wf	Working fluid

1. Introduction

Worldwide, the annual mean temperature is rising. To deal with this challenge, countries are committed to stabilize atmospheric greenhouse gas concentrations. Proposed strategies are based on a sustainable growth by means of greener and more efficient energy systems. In this regard, the Organic Rankine Cycle (ORC) is considered a promising technology to produce electricity from low-grade heat sources, even better than other exothermic engines [1]. Its operating principle is similar to the steam Rankine cycle, but using more volatile fluids instead of water to take profit from low-grade heat sources. Among ORC competitors for low-grade applications, the Kalina cycle highlights. However, the difference in performance shown experimentally with respect to the ORC was merely 3% better [2]. In addition, the ORC is significantly less complex and needs lower maintenance [3]. Therefore, the ORC adoption is currently being studied for numerous renewable and waste heat sources, such as geothermal [4], biomass [5], solar thermal [6], bottoming power cycles [7], industrial processes [8], oceanic [9], or other applications [10]. In particular, the ORC adoption for Waste Heat Recovery (WHR) from industrial processes has a great future potential of implantation [11]. Thus, a study conducted in the European Union (EU-27) estimated that an electrical power of 2.7 GW could be produced annually, saving 1,957 million euros and avoiding 8.1 million tons emissions to the atmosphere [12]. It must also be noted that over 50% of industrial heat rejections are considered as low-grade waste heat, whose temperatures do not exceed 300-350 ºC [13]. In most situations, the industries reject this low-grade heat because its recoverable energy is insufficient to offset transportation and reuse costs [14]. For this reason, the use of small-scale ORC systems, generally referred to systems that reach an electrical power up to 100 kW [15], for low-grade industrial WHR is considered as an improvement that may contribute with significant energy, environmental and economic benefits.

Regarding current investigations on the topic, they mainly have a technical character. Numerous studies are devoted to finding more efficient organic working fluids, as well as low Global Warming Potential (GWP) candidates for a drop-in replacement for HFC-245fa, which is the most popular fluid among commercial systems and whose GWP is 858 [16]. In this way, Huck *et al*. [17] concluded that the hydrochlorofluoroolefin HCFO-1233zd(E) is a promising alternative with a GWP of 1. Eyerer *et al*. [18] also proposed this fluid as drop-in replacement for HFC-245fa in existing ORC systems. The researchers argued that, in addition to the advantage of the low GWP, higher efficiency is reachable, but a slight reduction in electrical power occurs. Molés [19] also demonstrated experimentally that HCFO-1233zd(E) can be used as drop-in replacement for HFC-245fa, as well as the slight reduction in electrical power output. Moreover, the suitability of other low GWP candidates, such as the hydrofluoroolefins HFO-1234ze(Z) with a GWP of 1 and HFO-1336mzz(Z) with a GWP of 2, were theoretically assessed. Navarro-Esbrí *et al*. [20] experimentally confirmed the validity of the HFO-1336mzz(Z). Petr *et al*. [21] underlined the suitability of the HFO-1234ze(Z) due to their similar thermophysical properties to the HFC-245fa. In a similar way, Ziviani *et al*. [22] showed that HFO-1234ze(Z) achieves a slight increase in power output compared to HFC-245fa.

Many studies experimentally characterize the performance of different expansion technologies, which has been pointed out as a critical component to reach cost-effective solutions [64]. From a general point of view, volumetric (or positive displacement) machines are more appropriate than turbo-machines for micro and small-scale applications. This is because volumetric machines are characterized by lower flow rates, higher pressure ratios, much lower rotational speeds, besides to tolerate liquid phase during the expansion process [23]. On the other hand, turbo-machines are a more compact alternative from electrical power outputs of 70 kW [24]. Focusing on the application range of volumetric machines, different technologies can be distinguished. In this way, Lemort and Legros [25] established three categories according to the type of motion: orbital,

rotary, and reciprocant. Experimental investigations in each category can be found in literature [26].

Other investigations focused on technical issues, such as the architecture of the cycle [27], sizing of components like feed pump [28] or heat exchangers [29], or design of the control strategy adopted [30].

In spite of these technical advances, there is a lack of knowledge about experimental applications of small-scale ORC systems for WHR in industrial processes. This fact was underlined by Cavazzini *et al*. [31], who also highlighted the importance to develop models of commercial ORC systems, and to consider direct and indirect costs, in order to correctly evaluate the profitability of new industrial projects. The results revealed the unprofitability of the project, even with the use of the energy efficiency incentive. Nonetheless, researchers highlighted that an improvement in performance and investment cost could lead to more reliable solutions. The main reason for the lack of small-scale projects implemented within industries has been revealed due to the difficulty to reach profitable projects [24]. In fact, profitability is not guaranteed even with medium and large-scale projects [32].

Being aware of the economic feasibility relevance for the ORC adoption in practical applications, more cost-effective solutions are being explored in the literature through thermo-economic (a combination of thermodynamic and economic) optimizations [33]. This method of analysis consists of the system optimization according to cost-effective ratios, instead of just using performance ratios as objective functions [33]. Thus, the use of small-scale ORC systems in WHR applications better needs to be more cost-effective than efficient, as was reported by Tchanche *et al*. [34]. The reviewers demonstrated that results of optimizations focused on efficiency and cost-effective ratio do not match. Consequently, it was highlighted that the Specific Investment Cost (SIC) minimization is preferable than electrical power maximization for the ORC adoption. Tocci *et al*. [24] underlined that the lack of experimental applications and the scarce number of commercial systems in the small-scale range were due to the high value of SIC. The researchers concluded that in order to achieve competitive systems, ORC units should not exceed a SIC value of 3,500 €/kW for micro-scale applications (<10 kW) and 2,500 €/kW for small-scale applications (10 – 100 kW). However, these values are far from actual costs. For instance, Cavazzini *et al*. [31] estimated that the SIC of a small-scale project using a commercial 30 kW ORC was about 5,000 €/kW. In the medium-scale range, Lemmens *et al*. [35] reported a SIC of 4,216 €/kW_{gross} referred to a project using a 375 kW ORC to recover flue gas stream from an industrial plant. SIC values of large-scale plants range between 3,000 – 4,000 €/kW [36] . As it highlights, the lower the scale of the application, the less cost-effective is the SIC of the project.

With the aim to contribute to the adoption of small-scale ORC systems for industrial low-grade WHR, this paper proposes as novelty to conduct a thermo-economic optimization on the basis of an experimental application. Thereby, realistic results about the influence of geometric characteristics of the system (expander, heat exchangers, piping), architecture of the system, low GWP organic fluid used, or control strategy adopted can be assessed for the best cost-effective system and compared to the reference case.

For this purpose, the rest of the paper is organized as follows. Section 2 presents the case study and tests conducted. Section 3 describes the thermodynamic and economic models. Section 4 establishes the accuracy of the model through its calibration and validation from actual data of operation. Section 5 discusses the results of the study. And finally, Section 6 summarizes the main conclusions of the work.

2. Case of study

2.1. Facility description

The facility consisted of a pre-competitive ORC prototype, of a rated electrical power of 20 kW, installed in a ceramic kiln to take profit from the low-grade waste heat available in the exhaust air of the intermediate cooling zone. First tests with the facility were described in previous studies [37]. The main components of the system that require being modeled are shown in Fig. 1. There is a heat exchanger installed in the ceramic kiln to recover the waste heat (Fig. 1.a), and a heat transfer loop with thermal oil to transfers the heat recovered to the ORC module (Fig.1.b), which is located outdoors of the factory along with the air-cooled condenser (Fig. 1.c). Furthermore, details of the main components of the ORC such as the volumetric expansion machine, feed pump, or Heat Recovery Vapor Generator (HRVG) can be appreciated in Fig. 1.d. Among technical characteristics of the ORC module, it can be highlighted the use of a regenerative architecture, a subcritical thermodynamic cycle with superheating, HFC-245fa as organic fluid, a volumetric screw expander, and brazed plate heat exchangers.

Fig. 1. Photos of WHR system: (a) ceramic kiln and heat transfer loop; (b) recuperator installed in the heat source; (c) ORC module and condenser view; (d) internal detail of the module.

2.2. Monitoring

The main components of the WHR system are depicted in Fig. 2. This schematic also shows the parameters measured from the facility, as well as numbering used in the diagram of the thermodynamic cycle. Characteristics of metering devices, extracted from manufacturers' data sheets, are collected in Table 1. The uncertainty of the ratios analyzed in this manuscript is also calculated as a function of the uncertainty on each measured variable by Eq. (1) [38].

$$U_y = \sqrt{\sum_{i=1}^{N} \left(\frac{\partial y}{\partial x_i}\right)^2 \cdot U_{x_i}^2} \quad (1)$$

Fig. 2. Main components of the WHR system and monitoring parameters used.

Table 1. Information of metering devices.

2.3. Testing

With the aim to obtain performance data of the facility during typical operating conditions, the system was kept running for testing during a complete week. Thus, the monitored parameters of the reference case could be registered. The resolution of the registration was set per second, achieving more than 604,800 points of operation.

The industrial process is characterized by a stable behavior with smooth variations over time, allowing a steady-state model development. For the model validation, 21 steady-state points (three points per day) representative of the operating range were chosen. The selection was made averaging 15 minutes operation (900 direct measurements), and checking that mean absolute errors of all measurements remained below 5%, which is a value within the acceptable limits of the standard method for steady-state tests [39].

Measurements validation is represented by Fig. 3 that shows a comparison between the thermal power recovered in the heat source and the thermal power that finally reaches the organic fluid. First, the thermal power was measured in the duct of the exhaust air using temperature devices and a volumetric flow rate meter. Second, the thermal power that the ORC recovers was measured

on the organic fluid side using temperature, pressure and mass flow rate meters. As can be seen, deviation between both measurements occur, which is mainly due to heat losses in the heat transfer loop. Consequently, heat losses and pressure drops caused by the heat transfer loop are also included in the model.

Fig. 3. Comparison between thermal power recovered at the heat source and ORC module.

3. Modeling

The thermo-economic model should predict the net power output of the system, including all internal consumptions of the facility, as well as the investment cost of each component of the project. Thus, it can be conceptualized as two models, thermodynamic and economic.

3.1. Thermodynamic model

The performance of each component is modeled from the establishment of heat transfer and thermodynamics fundamentals and the definition of their geometric and control parameters. Submodels and their interconnection are depicted in Fig. 4. From a general point of view, this scheme represents the model capacity for the net electricity prediction from heat source and heat sink performance curves. The model is fed by thermophysical properties of the organic fluid, geometric parameters of the components used, and the control strategy implemented in the system. These feedings refer, firstly, to the actual values of the facility and, subsequently, they are optimized to simulate more profitable solutions. Different lines are shown in the schematic, which represent pipelines of the fluids, and electric lines for power or control purposes according to the figure legend. The components shown in the figure are classified as heat exchangers, fluid machines, and auxiliary components, which are addressed as follows.

Fig. 4. Scheme followed for the model development.

3.1.1. Heat exchangers

Waste heat can be recovered from the heat source by means of two different architectures. On the one hand, a direct heat exchanger between heat source and the organic fluid can be used. This configuration is considered more efficient and simpler, but involves numerous issues. Quoilin *et al.* [23] reported that, during start-up and transients, the working fluid may reach excessive temperatures for its chemical stability, even exceeding the decomposition temperature of the organic fluid when hot spots appear in the heat transfer area. On the other hand, waste heat can be indirectly recovered by using a heat transfer loop with thermal oil. This setup damps the heat source fluctuation, which improves the system controllability [40]. Consequently, this is the configuration that most commercial ORC systems adopt, such as the facility addressed in this study. A schematic of the indirect recuperator installed in the facility is depicted in Fig. 5.a. The exhausted air flows across the bank of finned tubes transferring the thermal power to the thermal oil. Accordingly, the thermal oil recovers this heat and leaves the recuperator at a higher temperature. Correlations used in the model of the recuperator are Eq. (2) proposed by Zukauskas [41] for the external flow of the entire tube bank with aligned tube rows arrangement, and Eq. (3) proposed by Gnielinski [42] for internal flow in tubes.

$$\mathrm{Nu} = 0.27 \cdot \mathrm{Re}_{\mathrm{max}}^{0.63} \cdot \mathrm{Pr}^{0.36} \cdot \left(\frac{\mathrm{Pr}}{\mathrm{Pr}_s}\right)^{0.25} \cdot 0.96 \quad (2)$$

$$Nu = \frac{\frac{f}{8} \cdot (Re - 1\,000) \cdot Pr}{1 + 12.7 \cdot \left(\frac{f}{8}\right)^{0.5} \cdot (Pr^{2/3} - 1)} \quad (3)$$

Heat rejection to the ambient can also be conducted by direct and indirect setups. The indirect setup can be driven by using a cooling water circuit between the condenser of the ORC and a dry cooler [20]. This configuration allows a smoother control of the condensing temperature. However, lower efficiencies can be reached by the ORC, since higher condensing temperatures occur compared to direct dissipation systems [23]. Furthermore, a more complex facility is required to implement a cooling-water circuit, including an extra pump with its corresponding consumption, and safety and control devices. Considering that high temperature issues do not occur in the dissipation process, and higher efficiencies are reachable by using a direct dissipation system [43], an air-cooled condenser is used in this facility. The air-cooled condenser consists of a bank of finned tubes, in which the organic fluid condenses inside the tubes and the ambient air is blown across the tubes through axial-flow fans. In particular, the device used consists of a horizontal unit with five fans in an induced-draft arrangement that is schematized in Fig. 5.b. The heat transfer on the air side of the condenser can be characterized through the correlation of Briggs and Young, shown in Eq. (4). This correlation has been extensively used for the flow of cooling air across triangular pitch banks of finned tubes [44]. The characteristics of the heat transfer mechanisms for condensation can be directly explained by Akers *et al*. correlation [45], presented in Eq. (5).

$$Nu = 0.134 \cdot Re_{max}^{0.681} \cdot Pr^{1/3} \cdot \left(\frac{r_{fin} - r_s}{Fin_{spacing}}\right)^{-0.2} \cdot \left(\frac{t_{fin}}{Fin_{spacing}}\right)^{-0.1134} \quad (4)$$

$$h = 5.03 \cdot Pr^{\frac{1}{3}} \cdot Re_l^{\frac{1}{3}} \cdot \frac{k}{D_i} \cdot \left(\frac{\chi}{1-\chi} \cdot \left(\frac{\rho_l}{\rho_v}\right)^{0.5} + 1\right) \quad (5)$$

Different brazed plate heat exchangers, formed by plates as shown in Fig. 5.c, are used inside the ORC module. The HRVG is composed of two heat exchangers, denoted as economizer and evaporator-superheater. The economizer works in the single-phase region, transforming subcooled liquid into practically saturated liquid. This heat exchanger has an initial heat transfer surface of 1.62 m^2. The evaporator continuously works in the two-phase region to achieve saturated vapor, but also in the single-phase region to feed the expander with superheated vapor. Both, single and two-phase correlations are used for the proper area calculation. This heat exchanger has an initial heat transfer surface of 5.28 m^2. In addition, the regenerator works in the single-phase region to exchange the sensible heat from the vapor side to the liquid side. This heat exchanger has an initial heat transfer surface of 12.9 m2. The single-phase correlation is used to model the economizer, regenerator, and the superheating part of the evaporator. The Eq. (6) was proposed by Sekhar V. [46] to model commercial brazed plate heat exchangers. The two-phase correlation is used for the evaporation process of the organic fluid. Dong *et al*. [47] proposed Eq. (7) for working fluids of ORC systems.

$$\frac{Nu}{Pr^y} = (C_0 + C_1 \cdot \beta + C_2 \cdot \beta^2) \cdot Re_c^{K_0 + K_1 \cdot \beta} + (C_3 + C_4 \cdot \beta + C_5 \cdot \beta^2) \cdot Re_c^{K_2 \cdot \beta} + C_6 \quad (6)$$

$$Nu = 2.64 \cdot Re_{eq}^{0.815} \cdot Pr_l^{0.333} \cdot Bo_{eq}^{0.343} \quad (7)$$

The adequacy of each correlation used was checked within their range of application. All complementary information about geometric parameters of heat exchangers and coefficients used in correlations are available according to Appendix A.

Fig. 5. Heat exchangers: (a) recuperator, transversal view of tubes; (b) induced-draft air-cooled condenser with two passes; (c) plate geometric parameters.

3.1.2. Fluid machines

Considering the isentropic transformation as the ideal thermodynamic expansion process, the actual expansion process can be modeled by considering irreversibilities that appear during this ideal transformation. Taking this into account, the model of the expander is depicted in Fig. 6, distinguishing between internal and external energy losses with respect to the limits of the expander. Internal energy losses depend on different performance ratios that can be independently modeled to improve the accuracy of the results [48]. One of the most relevant performance ratios is the volumetric efficiency, which is referred to internal leakages due to rotors and wall tolerances. This efficiency can be treated as a unique fictitious leakage path connecting the expander supply and exhaust [49]. It can be calculated as the relationship between the swept volume and the measured volumetric flow rate at the inlet port of the expander by Eq. (8). It can also be calculated inversely denoted as filling factor [50]. Under and over-expansion efficiency depends on the built-in volume ratio that is a geometric parameter defined as the relationship between discharge and swept volumes. Therefore, an off-design operation is considered an internal energy loss that can be quantified [51]. This efficiency is usually modeled as an isentropic expansion at the optimum ratio, along with an adiabatic expansion at constant volume, defined by Eq. (9) [49]. Mechanical losses are due to friction between moving elements, like screws or bearings, and internal pressure drops. The value of mechanical efficiency depends on the specific expander and its operating conditions. Thus, the higher the discharge volume and the lower the built-in volume ratio, the higher is the expander efficiency. This fact was pointed out by Astolfi [52], who proposed the regression of Eq. (10). Furthermore, other external losses also reduce the electrical power output. Specifically, there are mechanical losses due to the coupling between the shafts of expander and alternator, besides electrical losses in the conversion from mechanical to electrical power. Both, mechanical and electrical, losses can be considered in a single performance ratio, denoted as electro-mechanical efficiency by Eq. (11). Furthermore, as commonly is assumed in ORC models, the influence of the lubricating system over the performance ratios is considered negligible [53].

$$\eta_v = \frac{\dot{V}_{swept}}{\dot{V}_i} \tag{8}$$

$$\eta_{UnderOver} = \frac{\left(h_i - h_{V_r}\right) + 100/\rho_{V_r} \cdot \left(P_{V_r} - P_o\right)}{h_i - h_{o\,ise}} \tag{9}$$

$$\eta_{max} = 0.9403305 + 0.0293295 \cdot \ln\left(V_{discharge}\right) - 0.0266298 \cdot V_r \tag{10}$$

$$\eta_{em} = \frac{W_g}{\dot{m} \cdot (h_i - h_o)} \tag{11}$$

Fig. 6. Equivalent expander and energy losses.

Two pumps of the system require being modeled, the feed pump of the ORC and the thermal oil pump. The simplified method used for pumps modeling consists of its empirical performance calibration. For that, the feed pump is modeled by Eq. (12) using the overall performance of the pump. Moreover, the thermal oil pump is modeled by Eq. (13) assuming incompressible fluid conditions.

The last assumption was also used to model the electrical consumption of the fans from the condenser, and the increase of the industrial blower consumption due to the pressure drop caused by the recuperator. Regarding the condenser, the model also includes the effect of electrical consumption at partial loads calculation proposed by Chirakalwasan [54], allowing the simulation in a wide range of operating conditions.

$$\eta_{p} = \frac{\dot{m} \cdot (h_{o\,ise} - h_{i})}{W_{p}} \tag{12}$$

$$\eta_{oil_p} = \frac{\dot{V} \cdot (\Delta P \cdot 100)}{W_{oil\,p}} \tag{13}$$

3.1.3. Auxiliary components

There are more components that require being included in the model to conduct the optimization. Among them, highlight piping and fittings, the receiver included between the condenser and feed pump, or the control strategy adopted by the PID (Proportional-Integral-Derivative) controller.

More detailed information, including pressure drops, control strategy, and heat losses to the ambient calculations, is available in Appendix A. As a result, the net power output of the WHR system can be defined as the difference of gross power produced in the expander and electrical consumptions of feed pump, fans of the condenser, electronic devices, thermal oil pump, and industrial blower by Eq. (14).

$$W_{net} = W_{g} - W_{p} - W_{cond} - W_{other} - W_{oil\,p} - W_{blower} \tag{14}$$

3.2. Economic model

The economic model includes the cost of the main components of the whole facility. Cost correlations are collected in Table 2, which are adopted from literature on the basis of actual investment costs of the project.

Table 2. Cost correlations used in the economic model (€).

The sum of all costs of the project can be expressed in function of net power output, denoted as SIC of the project by Eq. (15), which is the variable used as objective function in the thermo-economic optimization.

$$SIC_{project} = \frac{C_{project}}{W_{net}} \tag{15}$$

4. Calibration and validation

4.1. Thermodynamic model

Some parameters related to the experimental performance of fluid machines and auxiliary components require being adjusted from actual data of operation to improve the model accuracy. Values used in the model, which are collected in Table 3, are obtained averaging those associated to the steady-state points.

Table 3. Summary of performance

Other parameters used in the calibration of the model refer to the part-load factor of the fans of the air-cooled condenser, and the equivalent length of vapor and liquid lines for the pressure drop calculation. This information, as well as the validation of each property measured, is detailed addressed in accordance with Appendix A. Nonetheless, the most important parameters are discussed below.

The exhaust air temperature that enters in the recuperator is the input of the model, but the temperature that leaves from it requires being validated. The results are illustrated in Fig. 7.a, which shows that all values are included in a bandwidth of 0.92%, excluding error bars. The mean absolute error was 0.36% and a standard deviation of 0.23% was obtained. These error values are proof of the model suitability to predict the thermal power recovered from the heat source. The thermal energy is transferred from the exhaust air to the thermal oil. Thus, the temperature of the thermal oil entering the ORC is validated in Fig. 7.b. The statistical analysis shows that values are within a bandwidth of 1.22%, excluding error bars, the mean absolute errors was 0.56%, and the standard deviations quantified was 0.31%. The temperatures of the organic working fluid entering and leaving from the expander are validated in Fig. 7.c and Fig. 7.d. Regarding the statistical analysis, all values are included in a bandwidth of 1.81% and 1.79% respectively, excluding error bars. The mean absolute errors were 0.45%, and 0.94%, and standard deviations of 0.54% and 1.01% were obtained, respectively.

The pressure is also a property measured in the circuit of the organic fluid. Different sensors are installed in the ORC unit to monitor high and low operating pressures, as well as to quantify the pressure drops in the circuit of the working fluid. The validation of the maximum pressure of the cycle, which corresponds to the outlet of the pump, is represented in Fig. 7.e. With respect to the statistical analysis, all values are included in a bandwidth of 1.40%, excluding error bars. The mean absolute error was 0.51%, and a standard deviation of 0.48% was obtained. Similarly, the prediction of the lower pressure measured in the cycle corresponds to the inlet pressure of the organic fluid into the condenser, validated in Fig. 7.f. The statistical analysis shows that all values are within a bandwidth of 2.03%, excluding error bars. The mean absolute error was 0.62% and a standard deviation of 0.85% was calculated.

The mass flow rate is a parameter measured at the liquid line of the circuit of the organic fluid. The validation of this parameter is shown in Fig. 7.g. Focusing on the statistical analysis, all values are included in a bandwidth of 2.79%, excluding error bars. The mean absolute error was 1.81%, and a standard deviation of 0.52% was calculated. The prediction of the organic working fluid mass flow rate is indicative of the small error assumed considering constant the volumetric efficiency of the expander.

The gross electrical power produced is validated in Fig. 7.h. The statistical analysis shows that all values are within a bandwidth of 3.52%, excluding error bars. The mean absolute error was 1.42%, and a standard deviation of 1.49% was obtained.

Fig. 7. Model validation with experimental data: (a) exhaust air temperature from recuperator; (b) inlet temperature of thermal oil into the ORC unit; (c) inlet temperature of organic fluid into the expander; (d) outlet temperature of organic fluid from the expander; (e) maximum pressure of the cycle; (f) inlet pressure of organic fluid into the condenser; (g) organic working fluid mass flow rate; (h) gross electrical power produced in the alternator.

4.2. Economic model

The economic results are collected in Table 4. The quantified cost is 55,417 € for the ORC unit (set of module and condenser) and 83,226 € for the whole WHR system. These results are very close to values previously reported based on the ORC supplier indications [55], accomplishing an

error about 5%. In light of this, the SIC value of the whole project referred to the case study is quantified as 6,747 €/kW.

Table 4. Calculated cost per component (€).

5. Results

Before conducting the multivariable optimization, some independent variables used in the system optimization are going to be separately assessed.

The first analysis deals with the superheating degree, which is the temperature difference between the input of the expander and saturated conditions. The superheating degree is an independent variable, which is adopted in the system as a setpoint value of the control system. In particular, the control of the ORC varies the mass flow rate, evaporating and condensing pressures and temperatures, and other dependent variables, to maintain the superheating degree close to the setpoint value established. This type of control is commonly used in ORC systems [19], whose value was predefined during the startup. This variable is typically minimized in the literature, usually considering a setpoint value of 5 K to ensure vapor quality at the inlet of the expander [56]. The main reason is due to the lower the superheating degree the higher the recovery capacity of the system. This effect can be appreciated in Fig. 8.a. Nonetheless, the electrical production reaches a maximum net electrical power with a superheating degree of 45 K, which allows a 1.6% SIC reduction by simply changing the control strategy adopted, as Fig. 8.b shows. This fact is due to the positive superheating influence when certain working fluids in a regenerative architecture are used, which is in accordance to literature [57].

The regenerator is the additional heat exchanger with respect to the conventional architecture of the cycle. This typology is also commonly discussed in the literature, since it allows improving the cycle efficiency, but not always the electrical power output [33]. Taking this into account, the influence of the regenerator is also assessed. For that, the exchange surface has been varied, such as Fig. 8.c shows. The results point out that the net electrical power tends to increase with the surface of the regenerator. Nonetheless, there is an optimum surface close to the value currently used in the facility that allows reducing the SIC of the project a 0.6%, as illustrates in Fig. 8.d.

In contrast to the optimized regenerator, the analysis of the condenser shows that it is oversized. The design decision was initially considered to minimize the electrical consumption of fans. However, Fig. 8.e demonstrates that electrical power almost does not vary until half of the tube length. It should be clarified that, despite a higher electrical consumption of fans is required with the tube length reduction, the electrical efficiency of the motors increases as it approaches to the rated conditions. So the electrical penalization is minimized. Consequently, a remarkable reduction of 13% in the SIC of the project is observed in Fig. 8.f, that drops to 5,853 €/kW.

Other main parameters investigated in the literature about the volumetric expansion technology is the influence of the built-in volume ratio over the cycle performance [58]. In this way, Fig. 8.g shows that there is a value that optimizes the performance of the expander and, hence, maximizes the electrical power output. In this case, the optimum value matches with that used in the reference case, such as Fig. 8.h shows.

Fig. 8. Individual parameters optimization: (a) Superheating degree; (b) $SIC_{project}$ assessment according to superheating degree; (c) Regenerator exchange surface; (d) $SIC_{project}$ assessment according to regenerator; (e) Condenser exchange surface; (f) $SIC_{project}$ assessment according to condenser; (g) Built-in volume ratio; (h) $SIC_{project}$ assessment according to built-in volume ratio.

The individual optimization of each parameter has shown that a more profitable system could be reached. However, the extent of improvement depends on the set of parameters. Consequently, a multivariable optimization is conducted considering geometric characteristics of the system (expander, heat exchangers, piping), architecture of the system, or control strategy adopted. Furthermore, and considering the growing effort to phase down the production and usage of HFCs [59], and in particular the HFC-245fa, more sustainable alternatives should be assessed. For that, drop-in alternatives investigated in the literature are used. Specifically, the fluid HCFC-1233zd(E) and HFO-1234ze(Z) were proposed due to their GWP of 1, besides their non-toxicity and minimum value of atmospheric lifetime [60].

For comparisons, different optimization strategies are analyzed in this investigation. First, the net power output of the system is used as objective function to be maximized. The results for the three working fluids considered are collected in Table 5. This table presents all the parameters used as independent variables, which are: control setpoints of the condenser and superheater; heat transfer area in function of the length of the condenser, number of tubes of the recuperator, and sizes of the HRVG and regenerator; volumetric flow rate of thermal oil; as well as expander geometric characteristics, like swept volume and built-in volume ratio.

The main results presented in this table show that all working fluids tend to recover the whole thermal power available in the heat source. For that, different values of the parameters are adopted. The results also show that the organic working fluid HCFO-1233zd(E) allows reaching the maximum net electrical power. However, due to the higher heat transfer area required, the cost-effective indicator SIC is the least profitable.

Table 5. Multi-variable optimization using the net electrical power maximization as objective function.

On the other hand, to achieve a cost-effective solution, the minimization of the $SIC_{project}$ is considered as objective function. As can be appreciated in Table 6, none of the optimizations use the whole thermal power available in the heat source. Nonetheless, substantially better values of $SIC_{project}$ are reached. The results also show that the organic working fluid HFO-1234ze(Z) can be used to achieve the most profitable solution. The thermodynamic cycle of the optimized system using $SIC_{project}$ as objective function is shown in Fig. 9.

Table 6. Multi-variable optimization using the SIC minimization as objective function.

Fig. 9. Thermodynamic cycle in a temperature-entropy diagram, minimizing the SIC of the project at rated operating conditions (numbering corresponds to Fig. 2).

According to these results, three scenarios can be distinguished in the optimization analysis: reference system of the case study, system with net electrical power maximized, and system with SIC minimized. Thus, Fig. 10.a shows these three scenarios with regard to electrical power produced and consumed. Firstly, it highlights that different solutions are obtained when power output or cost-effective ratios are used as objective function, which includes different components sizing and organic fluids selection. Both optimizations allow net power outputs higher than the reference case, being low GWP organic fluids suitable alternatives for the HFC-245fa replacement. Moreover, it has been demonstrated that there is a specific thermal power, different to the maximum available to be recovered, that optimizes the system. Thus, each industrial process will require its own thermo-economic analysis. Regarding electrical consumptions, the feed pump is the component that causes greatest reductions of power output. Thus, a more efficient feed pump could lead to more profitable systems. Paying attention to the scenario of net power maximization, a rise in electrical consumption of the industrial blower is observed, which

is due to the pressure drop caused by a larger recuperator. Regarding the scenario of SIC of the project minimization, it highlights that the size of the condenser tends to decrease causing a rise in fan consumption. Fig. 10.b depicts these three scenarios in function of costs of the components. As expected, the maximization of net power output impacts the investment cost of the project, prejudicing its economic feasibility. In contrast, the SIC of the project minimization leads to a more cost-effective project. Results show that, in general, the most expensive components are the recuperator and the condenser. In light of this, thermo-economic optimizations should encompass the entire project and not only the ORC unit. With the aim to improve future designs some features can be underlined. The components that require more attention to reduce their cost are the heat transfer loop, regenerator and, as expected, the expander and alternator. In contrast, components whose costs are less relevant to the project profitability are the economized, evaporator-superheater, feed pump, organic working fluid, and control system.

Fig. 10. Thermo-economic multi-variable optimization: (a) results in function of electrical power; (b) results in function of specific investment cost of the project.

As a general conclusion, the multivariable using the SIC minimization as objective function provides the most cost-effective solution. Accordingly, a comparison of the most relevant parameters of the optimized system and the reference case is shown in Table 7.

Table 7. Comparison between reference system used in the case study and system obtained from the thermo-economic optimization.

6. Conclusions

This paper has conducted a thermo-economic optimization of a small-scale ORC system for low-grade WHR based on an experimental case of application. A comprehensive model of the facility was developed, calibrated, and validated from actual data operation, revealing a suitable accuracy regarding electricity and costs estimation. For instance, the gross electrical power estimated by the model has been validated with an error bandwidth of 3.52%. Similarly, the error of investment cost estimations for the project was 5%.

The main conclusions obtained from the thermo-economic optimization can be summarized as follows:

- The multivariable optimization considering control strategies, geometric characteristics (heat exchangers, expander, piping), architecture of the system (regenerator, superheating) and low GWP organic fluid used has provided the most cost-effective solution. A reduction of the project investment cost from 83,227 € to 71,468 € was obtained and, at the same time, an increase of the overall process efficiency from 6.83% to 7.31 % was reached.
- It has been demonstrated that there is a specific thermal power, different to the maximum available to be recovered in the heat source, that optimizes the system. So a thermo-economic assessment to each application case is necessary. In particular, the averaged thermal power input was 180.6 kW for the reference case and 179.3 kW for the optimized system.
- The greater improvement achieved with respect to the reference case has been obtained by using a more compact direct air-cooled condenser, even in spite of the increase of fans electric consumption. Indeed, the length of the condenser was reduced from 9.5 m, of the reference case, to 5 m, of the optimized case.

- The greatest reduction of the electrical power output is due to the feed pump consumption. Nonetheless, due to the low significance over the SIC of the project, a more efficient component could be used to improve the results.
- The relevance of the costs of recuperator and condenser suggest that future thermo-economic optimizations should encompass the entire project and not only the ORC unit. Thus, the use of SIC of the project as objective function, instead of SIC of the ORC, is preferable. In this case, by means of the multivariable optimization, the SIC of the project dropped from 6,747 €/kW to 5,455 €/kW.
- Besides the recuperator and condenser, the components that require more attention to reduce their cost are the heat transfer loop, regenerator and, as expected, the expander and alternator. In contrast, components whose costs are less relevant on the project profitability are the economized, evaporator-superheater, feed pump, organic working fluid, and control system.

Future studies will include the effect of the working fluid and lubricating oil mixture over the system optimization. Moreover, it is planned to analyze the adoption of a liquid-cooled condenser for heat rejection, as well as the use of a direct thermal exchange between exhaust air and working fluid.

Appendix A

This manuscript is based on the work presented in the author's Ph.D. dissertation [61], which can be found online for complementary information at http://dx.doi.org/10.6035/14031.2017.221809.

Acknowledgments

The authors want to acknowledge the Jaume I University for its financial support under the Ph.D grant PREDOC/2013/28 of "Convocatòria d'ajudes predoctorals per a la formació de personal investigador del Pla de promoció de la investigació de la Universitat Jaume I de Castelló (Spain)". Also to thank greatly Rank®, the ORC manufacturer, for its contribution in this project.

References

[1] Casati EIM. New Concepts for Organic Rankine Cycle Power Systems. ISBN 978-94-6259-330-5. 2014.

[2] Chen H, Goswami DY, Stefanakos EK. A review of thermodynamic cycles and working fluids for the conversion of low-grade heat. Renew Sustain Energy Rev 2010;14:3059–67.

[3] Bombarda P, Invernizzi CM, Pietra C. Heat recovery from Diesel engines: A thermodynamic comparison between Kalina and ORC cycles. Appl Therm Eng 2010;30:212–9.

[4] Wang X, Levy EK, Pan C, Romero CE, Banerjee A, Rubio-Maya C, et al. Working fluid selection for organic Rankine cycle power generation using hot produced supercritical CO2 from a geothermal reservoir. Appl Therm Eng 2019;149:1287–304. doi:10.1016/j.applthermaleng.2018.12.112.

[5] Kalina J, Świerzewski M. Identification of ORC unit operation in biomass-fired cogeneration system. Renew Energy 2019;142:400–14. doi:10.1016/j.renene.2019.04.080.

[6] Arteconi A, Del Zotto L, Tascioni R, Cioccolanti L. Modelling system integration of a micro solar Organic Rankine Cycle plant into a residential building. Appl Energy 2019;251:113408. doi:10.1016/j.apenergy.2019.113408.

[7] Dragomir-Stanciu D. Improving the energy efficiency of a internal combustion engine cogeneration system using ORC as bottoming cycle. Procedia Manuf 2018;22:691–4. doi:10.1016/j.promfg.2018.03.099.

[8] Wei F, Senchuang G, Zhonghe H. Economic analysis of Organic Rankine Cycle (ORC) and Organic Rankine Cycle with internal heat exchanger (IORC) based on industrial waste heat source constraint. Energy Procedia 2019;158:2403–8. doi:10.1016/j.egypro.2019.01.291.

[9] Wang M, Jing R, Zhang H, Meng C, Li N, Zhao Y. An innovative Organic Rankine Cycle (ORC) based Ocean Thermal Energy Conversion (OTEC) system with performance simulation and multi-objective optimization. Appl Therm Eng 2018;145:743–54. doi:10.1016/j.applthermaleng.2018.09.075.

[10] Mahmoudi A, Fazli M, Morad MR. A recent review of waste heat recovery by Organic Rankine Cycle. Appl Therm Eng 2018;143:660–75. doi:10.1016/j.applthermaleng.2018.07.136.

[11] Southon M, Krumdieck S. Preliminary investigation into the current and future growth and affordability of ORC electricity generation systems. Proc. 3rd Int. Semin. ORC Power Syst., 2015, p. 1012–21.

[12] Campana F, Bianchi M, Branchini L, De Pascale A, Peretto A, Baresi M, et al. ORC waste heat recovery in European energy intensive industries: Energy and GHG savings. Energy Convers Manag 2013;76:244–52.

[13] Wang HT, Wang H, Zhang ZM. Optimization of Low-Temperature Exhaust Gas Waste Heat Fueled Organic Rankine Cycle. J Iron Steel Res Int 2012;19:30–6.

[14] Hnat G, Patten JS, Bartone LM, Cutting JC. Industrial Heat Recovery with Organic Rankine Cycles. Proc from Fourth Ind Energy Technol Conf 1982:524–32.

[15] Tchanche BF, Pétrissans M, G. Papadakis. Heat resources and organic Rankine cycle machines. Renew Sustain Energy Rev 2014;39:1185–99.

[16] Hodnebrog, Etminan M, Fuglestvedt JS, Marston G, Myhre G, Nielsen CJ, et al. Global warming potentials and radiative efficiencies of halocarbons and related compounds: A comprehensive review. Rev Geophys 2013;51:300–78.

[17] Huck P, Laursen AL, Zia J, Woolley L. Identification and test of Low Global Warming Potential Alternatives to HFC-245fa in Organic Rankine Cycles. ASME ORC, The Netherlands, 2013. 2013.

[18] Eyerer S, Wieland C, Vandersickel A, Spliethoff H. Experimental study of an ORC (Organic Rankine Cycle) and analysis of R1233zd-E as a drop-in replacement for R245fa for low temperature heat utilization. Energy 2016;103:660–71.

[19] Molés Ribera F. Doctoral thesis: “Análisis teórico y experimental de fluidos con bajo potencial de efecto invernadero como alternativas al HFC-245fa en ciclos orgánicos Rankine de baja temperatura”. University Jaume I of Castellon (Spain) 2015.

[20] Navarro-Esbrí J, Molés F, Peris B, Mota-Babiloni A, Kontomaris K. Experimental study of an Organic Rankine Cycle with HFO-1336mzz-Z as a low global warming potential working fluid for micro-scale low temperature applications. Energy 2017;133:79–89.

[21] Petr P, Raabe G. Evaluation of R-1234ze(Z) as drop-in replacement for R-245fa in

Organic Rankine Cycles - From thermophysical properties to cycle performance. Energy 2015;93:266–74.

[22] Ziviani D, Dickes R, Quoilin S, Lemort V. Organic Rankine cycle modelling and the ORCmKit library: analysis of R1234ze (Z) as drop-in replacement of R245fa for low-grade waste heat recovery. 29th Int Conf Effic Cost, Optim Simul Environ Impact Energy Syst 2016:1–13.

[23] Quoilin S, Broek M Van Den, Declaye S, Dewallef P, Lemort V. Techno-economic survey of organic rankine cycle (ORC) systems. Renew Sustain Energy Rev 2013;22:168–86.

[24] Tocci L, Pal T, Pesmazoglou I, Franchetti B. Small Scale Organic Rankine Cycle (ORC): A Techno-Economic Review. Energies 2017;10:413.

[25] Lemort V, Legros A. Positive displacement expanders for Organic Rankine Cycle systems. Org. Rank. Cycle Power Syst. Technol. Appl., Elsevier Ltd; 2016, p. 361–96.

[26] Rahbar K, Mahmoud S, Al-Dadah RK, Moazami N, Mirhadizadeh SA. Review of organic Rankine cycle for small-scale applications. Energy Convers Manag 2017;134:135–55.

[27] Peris B, Navarro-Esbrí J, Molés F. Bottoming organic Rankine cycle configurations to increase Internal Combustion Engines power output from cooling water waste heat recovery. Appl Therm Eng 2013;61:364–71.

[28] Bianchi G, Fatigati F, Murgia S, Cipollone R, Contaldi G. Modeling and Experimental Activities on a Small-scale Sliding Vane Pump for ORC-based Waste heat Recovery Applications. Energy Procedia 2016;101:1240–7.

[29] Lazova M, Huisseune H, Kaya A, Lecompte S, Kosmadakis G, De Paepe M. Performance Evaluation of a Helical Coil Heat Exchanger Working under Supercritical Conditions in a Solar Organic Rankine Cycle Installation. Energies 2016;9:432.

[30] Hernandez A, Desideri A, Ionescu C, Quoilin S, Lemort V, De Keyser R. Increasing the efficiency of Organic Rankine Cycle Technology by means of Multivariable Predictive Control. vol. 47. IFAC; 2014.

[31] Cavazzini G, Dal Toso P. Techno-economic feasibility study of the integration of a commercial small-scale ORC in a real case study. Energy Convers Manag 2015;99:161–75.

[32] Battisti L, Cozzini M, Macii D. Industrial Waste Heat Recovery Strategies in Urban Contexts: a Performance Comparison. Smart Cities Conf (ISC2), 2016 IEEE Int 2016.

[33] Quoilin S, Declaye S, Tchanche BF, Lemort V. Thermo-economic optimization of waste heat recovery Organic Rankine Cycles. Appl Therm Eng 2011;31:2885–93.

[34] Tchanche. BF, Quoilin. S, Declaye. S, Papadakis. DG, Lemort. V. Economic Optimization of small scale organic rankine cycles. 23rd Int Conf Effic Cost, Optim Simul Environ Impact Energy Syst 2010.

[35] Lemmens S, Lecompte S. Case study of an organic Rankine cycle applied for excess heat recovery: Technical, economic and policy matters. Energy Convers Manag 2017;138:670–85.

[36] Forni D, Vaccari V, Santo D Di, Baresi M. Heat recovery for electricity generation in industry 2012:523–34.

[37] Peris B, Navarro-Esbrí J, Molés F, Mota-Babiloni A. Experimental study of an ORC (organic Rankine cycle) for low grade waste heat recovery in a ceramic industry. Energy 2015;85:534–42.

[38] Lemort V, Quoilin S, Cuevas C, Lebrun J. Testing and modeling a scroll expander integrated into an Organic Rankine Cycle. Appl Therm Eng 2009;29:3094–102.

[39] Standard practice for calculating thermal transmission properties under steady-state sonditions. Annu B ASTM Stand 2012;14:1–13.

[40] Jiménez-Arreola M, Wieland C,Romagnoli A. Direct vs indirect evaporation in Organic Rankine Cycle (ORC) systems: A comparison of the dynamic behavior for waste heat recovery of engine exhaust. Appl Therm Eng 2019;242:439–452.

[41] Zukauskas, A., "Convective Heat Transfer in Cross Flow," in S. Kakac, R. K. Shah, and W. Aung, Eds., Handbook of Single-Phase Convective Heat Transfer, Wiley, New York, 1987. n.d.

[42] Incropera F, Dewitt D. Fundamentals of Heat and Mass Transfer. 7th edition. ISBN: 978-0470-50197-9. n.d.

[43] Application Of The Novel "Emeritus" Air Cooled Condenser In Geothermal ORC. Energy Procedia 2017;129:479-486.

[44] Briggs, D. E. and E. H. Young, Convection heat transfer and pressure drop of air flowing across triangular pitch banks of finned tubes, Chem. Eng. Prog. Symp. Ser., 59, No. 41, 1–10, 1963. n.d.

[45] Xiaoyong WEI, Xiande F, Rongrong SHI. A Comparative Study of Heat Transfer Coefficients for Film Condensation. Energy Sci Technol 2012;3:1–9.

[46] Sekhar Gullapalli V. Doctoral Thesis. Estimation of Thermal and Hydraulic Characteristics of Compact Brazed Plate Heat Exchangers. Lund University, Sweden. 2013.

[47] Junqi D, Xianhui Z, Jianzhang W. Experimental investigation on heat transfer characteristics of plat heat exchanger applied in organic Rankine cycle (ORC). Appl Therm Eng 2017;112:1137–52.

[48] Imran M, Usman M, Park BS, Lee DH. Volumetric expanders for low grade heat and waste heat recovery applications. Renew Sustain Energy Rev 2016;57:1090–109.

[49] Lemort V, Declaye S, Quoilin S. Experimental characterization of a hermetic scroll expander for use in a micro-scale Rankine cycle. Proc Inst Mech Eng Part A J Power Energy 2012;226:126–36.

[50] Zanelli R, Favrat D. Experimental investigation of a hermetic scroll expander-generator. 12th Int Compress Eng Conf Purdue 1994:459–64.

[51] Lei B, Wang W, Wu Y-T, Ma C-F, Wang J-F, Zhang L, et al. Development and experimental study on a single screw expander integrated into an Organic Rankine Cycle. Energy 2016;116:43–52.

[52] Astolfi M. Techno-economic Optimization of Low Temperature CSP Systems Based on ORC with Screw Expanders. Energy Procedia 2015;69:1100–12.

[53] Minea V. Power generation with ORC machines using low-grade waste heat or renewable energy. Appl Therm Eng 2014;69:143–54.

[54] Chirakalwasan R. Motor load and efficiency. ASHARE J 2006 - 2007 n.d.:21–33.

[55] Navarro-Esbrí J, Peris B, Collado R, Molés F. Micro-generation and micro combined heat and power generation using "free" low temperature heat sources through Organic Rankine Cycles. Renew Sustain Energy Rev 2013;16 (2012):4175–4189.

[56] Lecompte S, Lemmens S, Huisseune H, Van Den Broek M, De Paepe M. Multi-objective thermo-economic optimization strategy for ORCs applied to subcritical and transcritical cycles for waste heat recovery. Energies 2015;8:2714–41.

[57] Algieri A, Morrone P. Comparative energetic analysis of high-temperature subcritical and transcritical Organic Rankine Cycle (ORC). A biomass application in the Sibari district. Appl Therm Eng 2012;36:236–44.

[58] Zhu Y, Jiang L, Jin V, Yu L. Impact of built-in and actual expansion ratio difference of expander on ORC system performance. Appl Therm Eng 2014;71:548–58. doi:10.1016/j.applthermaleng.2014.07.024.

[59] UN Environment. Kigali Amendment. <Available in: www.unep.org> [accessed 01.05.2017] n.d.

[60] Navarro-Esbría J, Peris B, Molés F, Mota-Babilonia A, Barragán-Cerveraa Á. Theoretical Optimization of High Temperature Heat Pumps (HTHP) using Low GWP working fluids. The 4th International Symposium Waste heat valorization in industrial processes. 23-24 May 2016, Kortrijk, Belgium. Evolution (N Y) 2016.

[61] Peris Pérez B. Doctoral Thesis. Thermo-economic assessment of small-scale organic Rankine cycle for low-grade industrial waste heat recovery based on an experimental application. Jaume I de Castelló, 2017. doi:10.6035/14031.2017.221809.

[62] Astolfi M, Romano M, Bombarda P, Macchi E. Binary ORC (Organic Rankine Cycles) power plants for the exploitation of medium-low temperature geothermal sources 2014;66:435–46.

[63] Rettig A, Müller U, Sergi T. Exemplary Thermodynamic Assessment of a small ORC Application using dynamic Simulations. 3rd Engine ORC Consort Work 2016, Belfast, North Ireland n.d.

[64] Collings P, Yu Z, Wang E. A dynamic organic Rankine cycle using a zeotropic mixture as the working fluid with composition tuning to match changing ambient conditions. Appl Energy 2016;171:581–91.

[65] Lecompte S, Huisseune H, van den Broek M, De Schampheleire S, De Paepe M. Part load based thermo-economic optimization of the Organic Rankine Cycle (ORC) applied to a combined heat and power (CHP) system. Appl Energy 2013;111:871–81.

[66] Nusiaputra Y, Wiemer H-J, Kuhn D. Thermal-Economic Modularization of Small, Organic Rankine Cycle Power Plants for Mid-Enthalpy Geothermal Fields. Energies 2014;7:4221–40.

Fig. 1. Photos of WHR system: (a) ceramic kiln and heat transfer loop; (b) recuperator installed in the heat source; (c) ORC module and condenser view; (d) internal detail of the module.

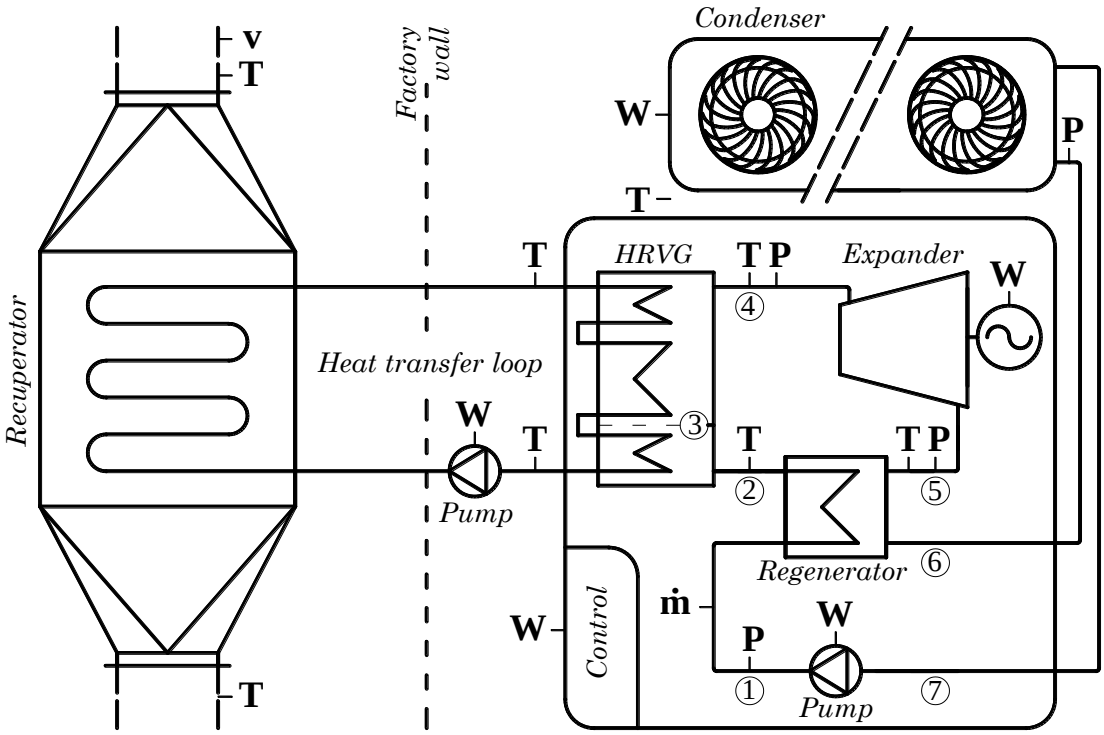

Fig. 2. Main components of the WHR system and monitoring parameters used.

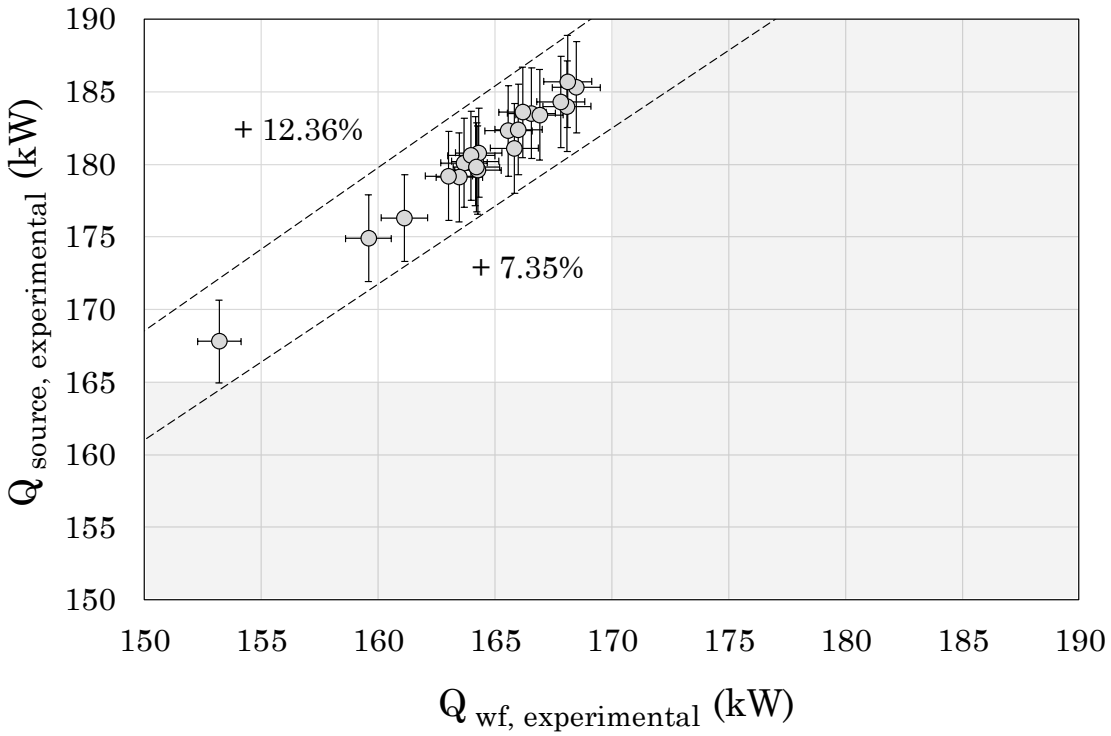

Fig. 3. Comparison between thermal power recovered at the heat source and ORC module.

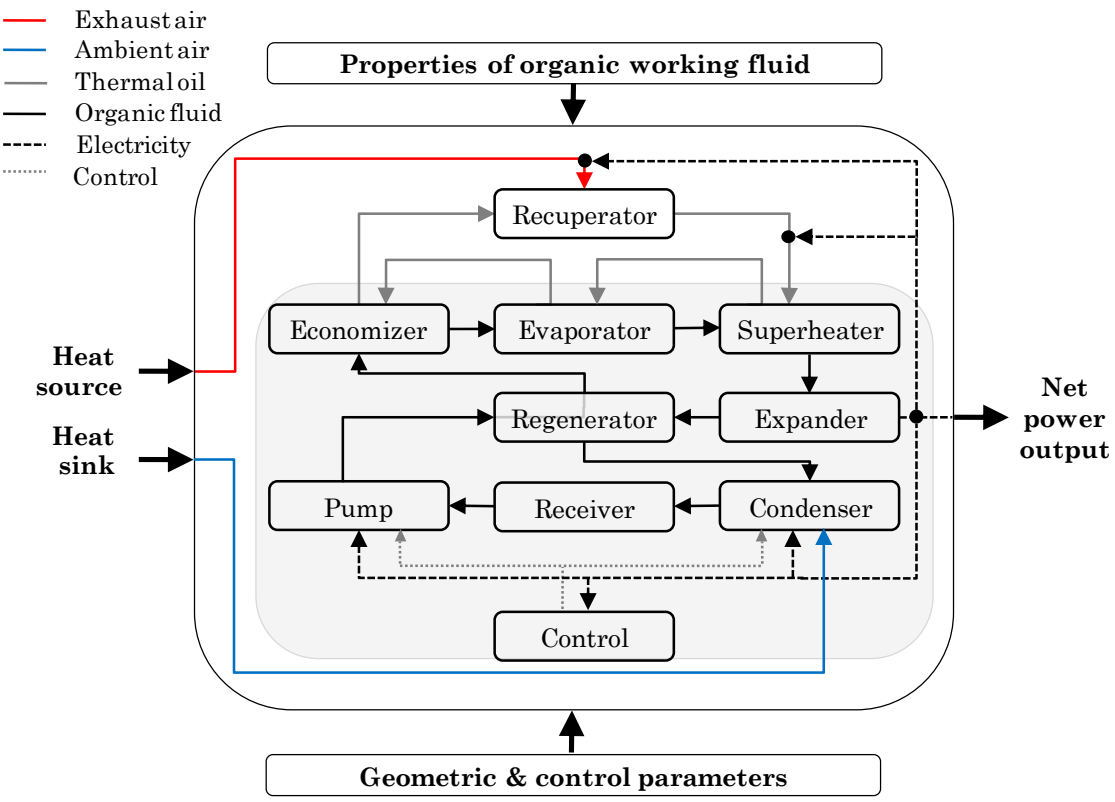

Fig. 4. Scheme followed for the model development.

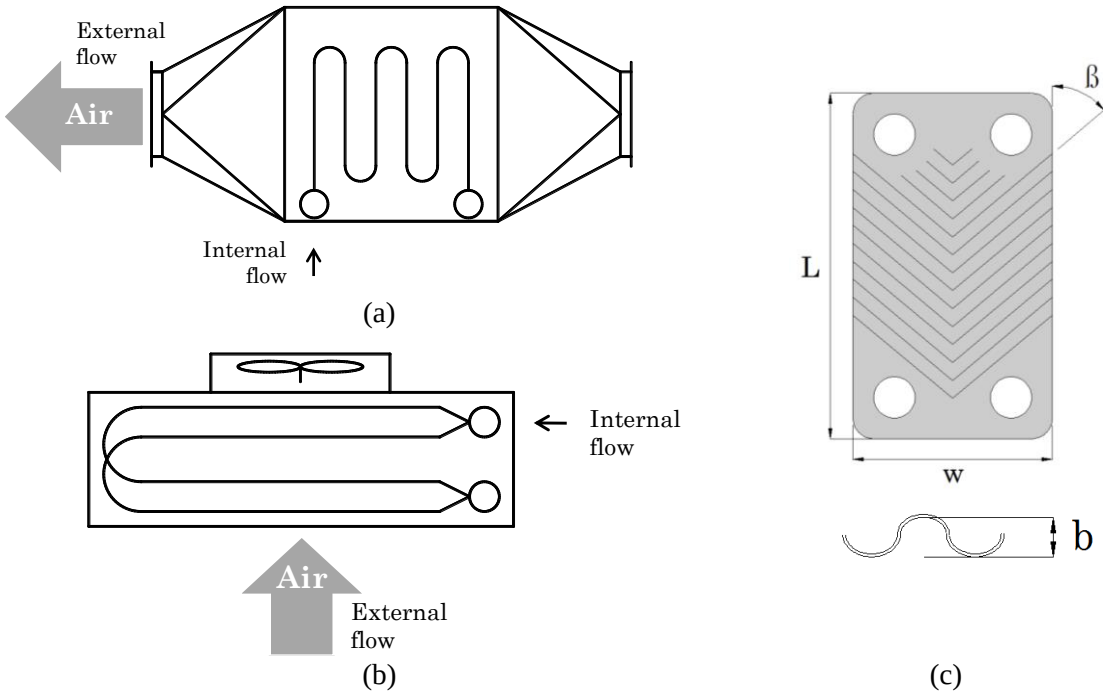

Fig. 5. Heat exchangers: (a) recuperator, transversal view of tubes; (b) induced-draft air-cooled condenser with two passes; (c) plate geometric parameters.

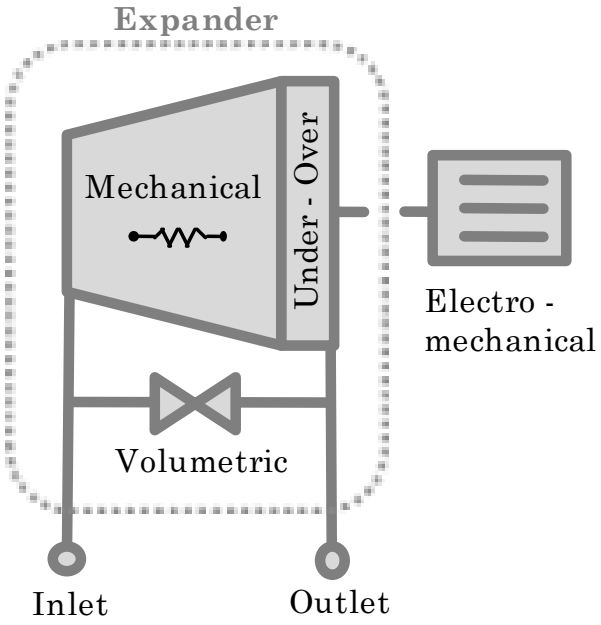

Fig. 6. Equivalent expander and energy losses.

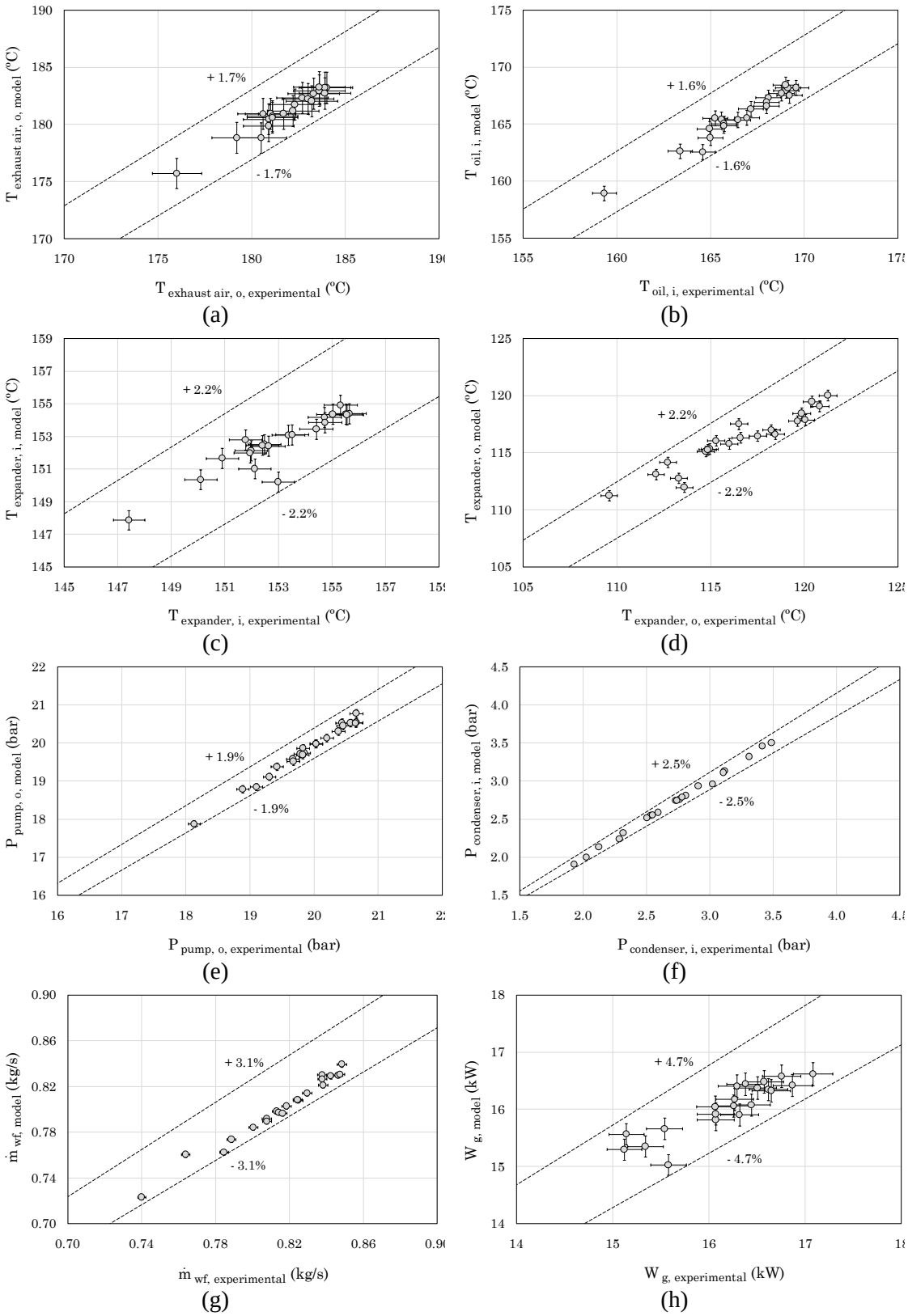

Fig. 7. Model validation with experimental data: (a) exhaust air temperature from recuperator; (b) inlet temperature of thermal oil into the ORC unit; (c) inlet temperature of organic fluid into the expander; (d) outlet temperature of organic fluid from the expander; (e) maximum pressure of the cycle; (f) inlet pressure of organic fluid into the condenser; (g) organic working fluid mass flow rate; (h) gross electrical power produced in the alternator.

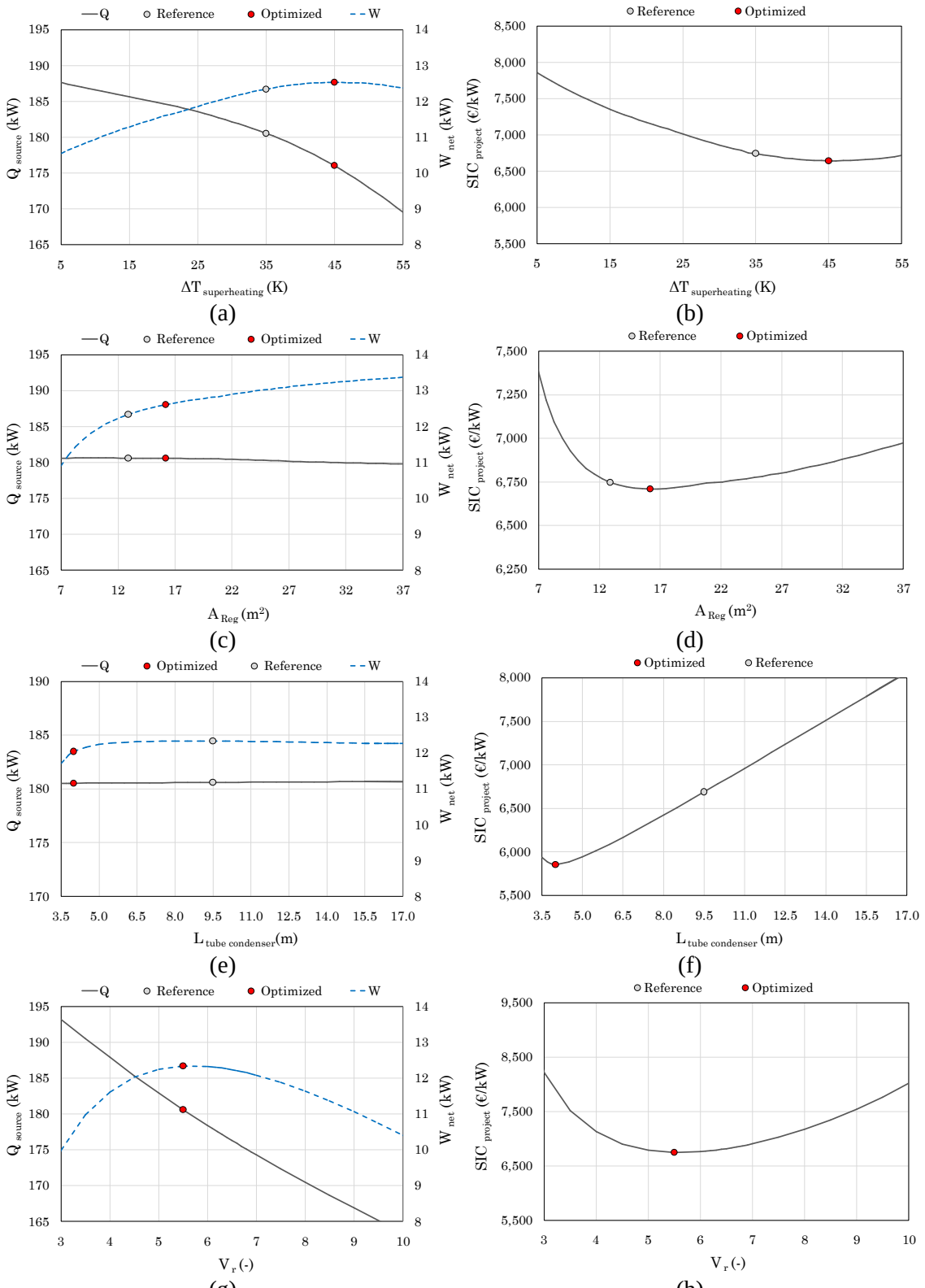

Fig. 8. Individual parameters optimization: (a) Superheating degree; (b) $SIC_{project}$ assessment according to superheating degree; (c) Regenerator exchange surface; (d) $SIC_{project}$ assessment according to regenerator; (e) Condenser exchange surface; (f) $SIC_{project}$ assessment according to condenser; (g) Built-in volume ratio; (h) $SIC_{project}$ assessment according to built-in volume ratio.

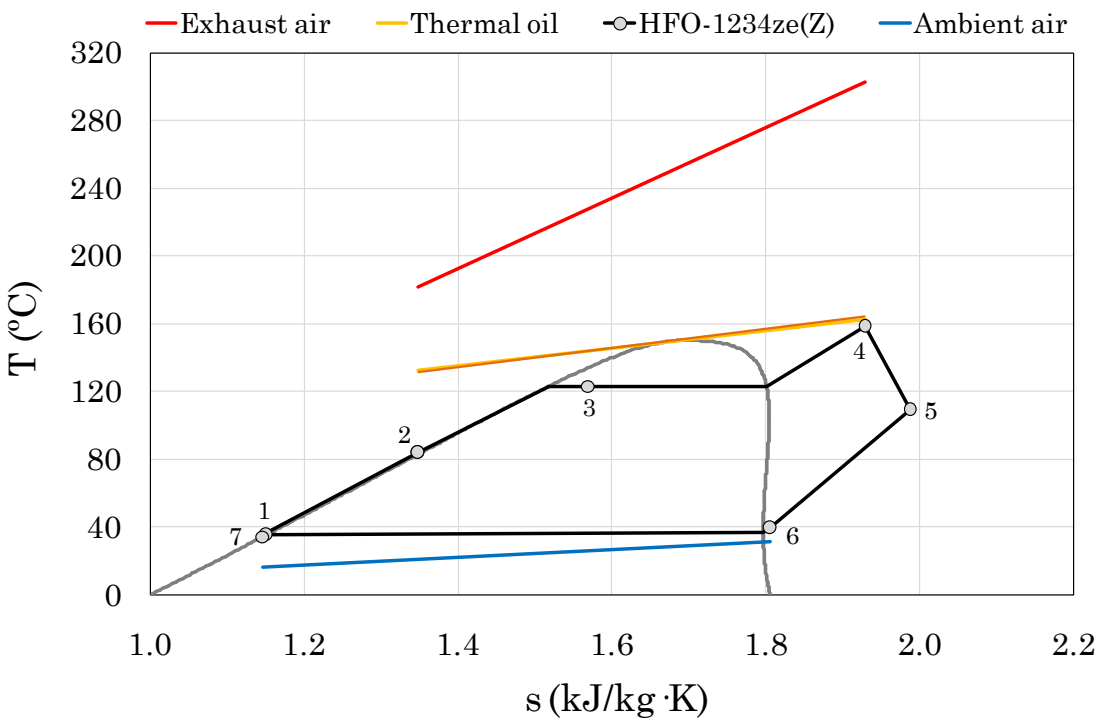

Fig. 9. Thermodynamic cycle in a temperature-entropy diagram, minimizing the SIC of the project at rated operating conditions (numbering corresponds to Fig. 2).

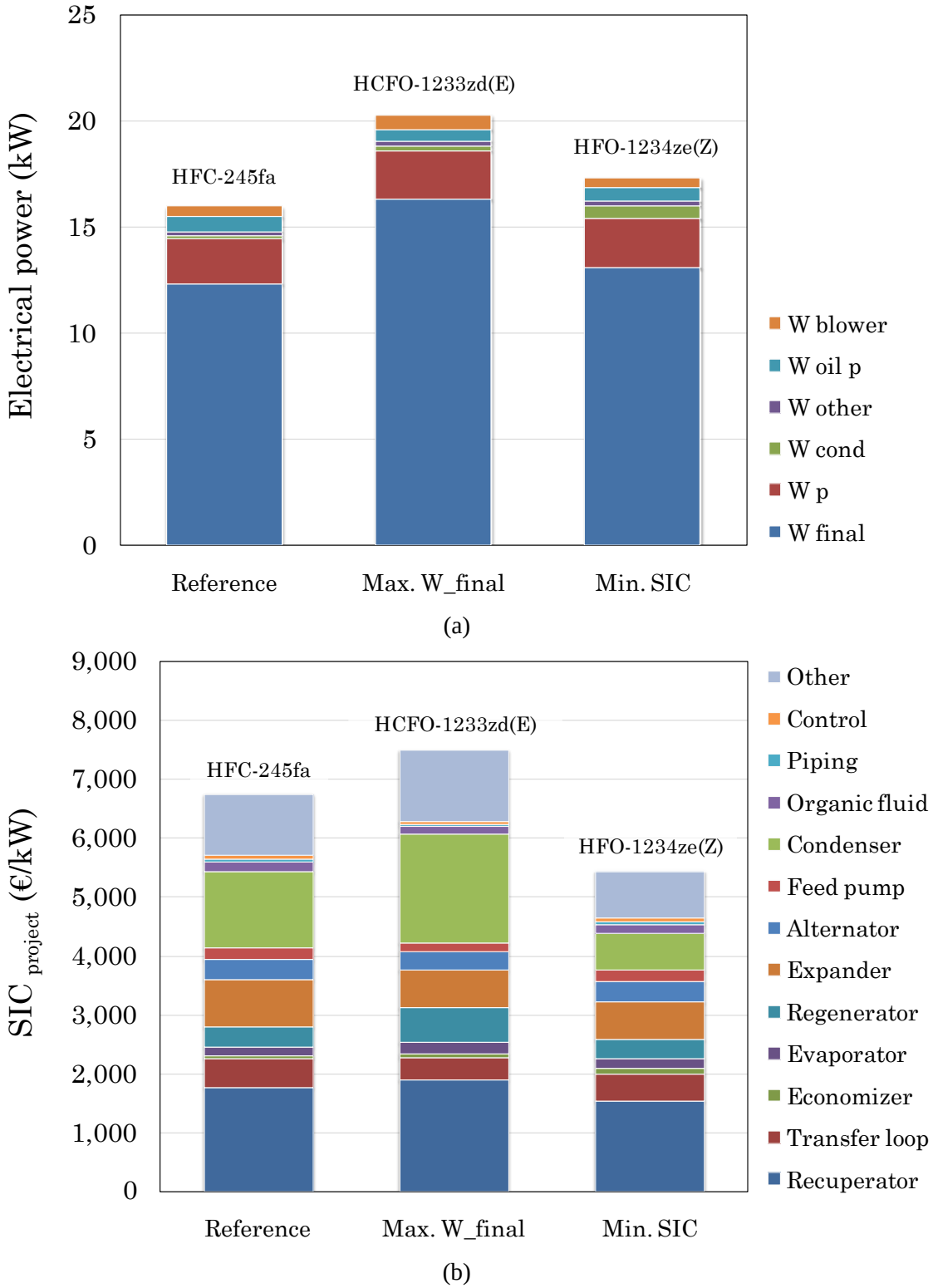

Fig. 10. Thermo-economic multi-variable optimization: (a) results in function of electrical power; (b) results in function of specific investment cost of the project.

Figure captions

Fig. 1. Photos of WHR system: (a) ceramic kiln and heat transfer loop; (b) recuperator installed in the heat source; (c) ORC module and condenser view; (d) internal detail of the module.

Fig. 2. Main components of the WHR system and monitoring parameters used.

Fig. 3. Comparison between thermal power recovered at the heat source and ORC module.

Fig. 4. Scheme followed for the model development.

Fig. 5. Heat exchangers: (a) recuperator, transversal view of tubes; (b) induced-draft air-cooled condenser with two passes; (c) plate geometric parameters.

Fig. 6. Equivalent expander and energy losses.

Fig. 7. Model validation with experimental data: (a) exhaust air temperature from recuperator; (b) inlet temperature of thermal oil into the ORC unit; (c) inlet temperature of organic fluid into the expander; (d) outlet temperature of organic fluid from the expander; (e) maximum pressure of the cycle; (f) inlet pressure of organic fluid into the condenser; (g) organic working fluid mass flow rate; (h) gross electrical power produced in the alternator.

Fig. 8. Individual parameters optimization: (a) Superheating degree; (b) SICproject assessment according to superheating degree; (c) Regenerator exchange surface; (d) SICproject assessment according to regenerator; (e) Condenser exchange surface; (f) SICproject assessment according to condenser; (g) Built-in volume ratio; (h) SICproject assessment according to built-in volume ratio.

Fig. 9. Thermodynamic cycle in a temperature-entropy diagram, minimizing the SIC of the project at rated operating conditions (numbering corresponds to Fig. 2).

Fig. 10. Thermo-economic multi-variable optimization: (a) results in function of electrical power; (b) results in function of specific investment cost of the project.

Table 1. Information of metering devices.

Parameter		Use	Instrument	Accuracy (%)	Range
Temperature	T	ORC Recuperator	Thermocouple PT-100	± 0.4 ± 0.75	0 – 750 ºC -100 +450 ºC
Pressure	P	ORC	Transmitter	± 0.5	0 – 40 bar
Mass flow rate	ṁ	ORC	Coriolis flow meter	± 0.3	< 6500 kg/h
Velocity	v	Recuperator.	Gas analyzer	± 1.5	-
Electricity	W	ORC Other	Wattmeter Grid analyzer	± 1.2 ± 0.2	- < 80 kW

Table 2. Cost correlations used in the economic model (€).

ORC module		
Twin-screw expander	$C_{screw} = (3\,143.7 + 217\,423 \cdot \dot{V}_{discharge}) \cdot USD$	[50]
Alternator	$C_{alternator} = 2x10^5 \cdot \left(\frac{W_g}{5000}\right)^{0.67}$	[60]
Brazed Plate Heat exchangers	$C_{BPHE} = 190 + 310 \cdot A$	[33]
Feed pump	$C_{pump} = (1\,970 \cdot {W_p}^{0.35}) \cdot USD$	[61]
Organic working fluid	$M = 5.05 \cdot W_g$	[62]
	$C_{wf} = 20 \cdot M$	[63]
Condenser	$C_{condenser} = (5.6 \cdot A) \cdot USD$ $C_{fans} = (1\,887.5 + 159.95 \cdot {D_{fans}}^2 + 3.53 \cdot D_{fans} + 281.25 \cdot W_{e\,fan}) \cdot N_{fans} \cdot USD$	[34]
Piping	$C_{piping} = (-6.90 + 675 \cdot D_{piping}) \cdot L_{piping}$	[63]
Other	$C_{other} = 0.3 \cdot C_{ORC}$ $C_{control} = 800$	[64]
Recuperator	$C_{recuperator} = 228 \cdot A$	
Heat transfer loop	$C_{htl} = 6{,}000$	

Table 3. Summary of performance

Fluid machine	**Empirical efficiency (%)**
Expander efficiency	
Volumetric	75.3
Mechanical (internal)	75.07
Electro-mechanical (external)	93.8
Pumps efficiency	
Feed pump	48.02
Thermal oil	40.45

Table 4. Calculated cost per component (€).

Cost of expander	9,881
Cost of electric generator	4,260
Cost of brazed plate economizer	692
Cost of brazed plate evaporator	1,827
Cost of brazed plate regenerator	4,189
Cost of feed pump of the ORC	2,413
Cost of organic working fluid	2,020
Cost of heat exchange surface of the condenser	5,858
Cost of the five fans of the condenser	10,092
Cost of pipes of organic fluid circuit	596
Cost of control and miscellaneous hardware	800
Cost of other components	12,789
Cost of recuperator	21,809
Cost of heat transfer loop	6,000

Table 5. Multi-variable optimization using the net electrical power maximization as objective function.

	HFC-245fa	**HCFO-1233zd(E)**	**HFO-1234ze(Z)**
Independent variables			
$\Delta T_{condensing}$ (K)	16	18.9	20
$\Delta T_{superheating}$ (K)	43.2	40.7	42.8
$L_{tube\ condenser}$ (m)	14	18	12
$N_{Recuperator}$ (−)	16	20	16
A_{HRVG} (m^2)	11.2	12.9	11.4
A_{Reg} (m^2)	26.3	30.8	23.7
$\dot{V}_{oil}$ (m^3/h)	10.0	8.6	9.93
$\dot{V}_{swept}$ (m^3/h)	31.01	30.08	30.09
V_r (−)	4.77	4.40	4.24
Main results			
Q_{source} (kW)	196.6	196.6	196.6
W_{net} (kW)	15.96	16.33	15.70
$\eta_{process}$ (%)	8.1	8.3	8.0
$SIC_{project}$ (€/kW)	6,639	7,499	6,275

Table 6. Multi-variable optimization using the SIC minimization as objective function.

	HFC-245fa	**HCFO-1233zd(E)**	**HFO-1234ze(Z)**
Independent variables			
$\Delta T_{condensing}$ (K)	25.2	20.8	20
$\Delta T_{superheating}$ (K)	33.9	35.4	35.1
$L_{tube\ condenser}$ (m)	4.0	4.5	5.0
$N_{Recuperator}$ (−)	13	13	13
A_{HRVG} (m^2)	10.5	10.3	10.1
A_{Reg} (m^2)	14.2	15.0	13.7
$\dot{V}_{oil}$ (m^3/h)	10.0	9.6	10.0
$\dot{V}_{swept}$ (m^3/h)	20.89	22.45	21.26
V_r (−)	4.6	4.7	4.6
Main results			
Q_{source} (kW)	178.5	172.1	179.3
W_{net} (kW)	12,41	12.51	13.10
$\eta_{process}$ (%)	7.0	7.3	7.3
$SIC_{project}$ (€/kW)	5,597	5,734	5,455

Table 7. Comparison between reference system used in the case study and system obtained from the thermo-economic optimization.

	Reference	Optimized
Economic indexes		
Project SIC (€/kW)	6,747	5,455
ORC SIC (€/kW)	3,997	3,018
Project investment cost (€)	83,227	71,468
System performance		
Thermal power input (kW)	180.61	179.3
Thermal power output (kW)	147.70	144.20
Net power output (kW)	12.34	13.10
ORC power output (kW)	17.52	19.20
Cycle efficiency (%)	9.7	10.7
Process efficiency (%)	6.83	7.31
Thermodynamic properties		
Organic working fluid (-)	HFC-245fa	HFO-1234ze(Z)
Organic fluid mass flow rate (kg/s)	0.79	0.71
Evaporating temperature (ºC)	118.50	123.20
Condensing temperature (ºC)	39.53	35.43
Expander inlet temperature (ºC)	152.28	158.23
Expander inlet pressure (bar)	18.57	21.47
Pressure ratio in expander (-)	5.75	7.57
Pressure ratio in pump (-)	6.90	6.94
Subcooling degree (K)	5.39	5.07
Components performance		
Expander isentropic efficiency (%)	56.0	54.1
Regenerator effectiveness (%)	91.9	93.8
Recuperator effectiveness (%)	70.5	70.6
Pinch Point in heat HRVG (K)	20.49	17.93
Pinch Point in condenser (K)	3.17	5.04
Pressure drop in exhaust air (bar)	1.7E-03	1.6E-03
Pressure drop thermal oil circuit (bar)	1.13	0.96
Pressure drop in ORC liquid lines (bar)	1.07	0.18
Pressure drop in ORC vapor lines (bar)	0.57	0.48
Thermal oil volumetric flow rate (m^3/h)	9.07	10.0
Components geometric characteristics		
Expander built-in volume ratio	5.5	4.6
Swept volume of expander (m^3/h)	22.2	21.26
Exchange surface of HRVG (m^2)	6.9	10.1
Exchange surface of regenerator (m^2)	12.9	13.7
Length of condenser (m)	9.5	5.0